Hierarchical porous $ZnMn_2O_4$ derived from cotton substance as high-performance lithium ion battery anode

Chenhao Zhao[1,2] ✉, *Ye Shen*[1], *Sheng'en Qiu*[1], *Zhibiao Hu*[1,2], *Kaiyu Liu*[1,2]

[1]*College of Chemistry and Materials Science, LongYan University, Fujian LongYan 364012, People's Republic of China*
[2]*Fujian Provincial Key Laboratory of Clean Energy Materials, LongYan University, Fujian LongYan, 364012, People's Republic of China*
✉ *E-mail: Zhaochenhao123456@163.com*

Published in Micro & Nano Letters; Received on 22nd February 2016; Accepted on 23rd March 2016

Hierarchical porous $ZnMn_2O_4$ has been prepared by an initial cotton template and subsequent calcination route. The as-prepared hierarchical porous $ZnMn_2O_4$ composed of numerous nanoparticles well inherit the fibre-like structure of cotton, and these nanoparticles have a size of ~20–50 nm. The N_2 adsorption–desorption test indicates this $ZnMn_2O_4$ has a Brunauer–Emmett–Teller surface area of ~16.7084 $m^2\ g^{-1}$ and average pore size of ~27.0 nm. As lithium ion battery anodes, the $ZnMn_2O_4$ can deliver a discharge capacity of 674.9 mAh g^{-1} after 200 cycles at current density of 200 mA g^{-1}. Even at 1000 mA g^{-1}, this $ZnMn_2O_4$ still shows a stable discharge capacity of 541.5 mAh g^{-1}. These promising electrochemical performances may be attributed to its unique hierarchical porous structure which helps to accelerate the ions transportation and elevate the structure stability.

1. Introduction: To meet the increasing requirement of lithium ion battery with high discharge capacity, high energy density and good cycling stability, the development of high-capacity anode materials need to be intensively carried out compared with commercial carbon-based anode [1–4]. Recently, the $ZnMn_2O_4$ has been considered as one of promising anode materials for LIBs due to its high reversible capacities (500–900 mAh g^{-1}), relatively good cycling stability and low cost. Especially, the manganese-based oxides such as $ZnMn_2O_4$ have lower operating voltage compared with other cobalt or iron based oxides, and a lower voltage is favourable to give more energy at a whole cell as anode materials [5–13].

As conversion-typed anode, the practice use of $ZnMn_2O_4$ is also prevented by the serve volume change during cycling, resulting in unnecessary capacity fading. In order to alleviate this problem, one of effective strategies is to design and preparation of porous structural $ZnMn_2O_4$. Therein, the introduced void space in porous structure can buffer the volume change, facilitate a close contact with electrolyte and accelerate the diffusion of lithium ions, and an improved electrochemical performance can be expected [14, 15]. For example, Qian *et al*. had prepared porous $ZnMn_2O_4$ microspheres by decomposition of corresponding Zn-Mn binary carbonate. The as-prepared porous microspheres can preserve a discharge capacity of 800 mAh g^{-1} at current density of 500 mA g^{-1} after 300 cycles [16].

The natural cellulose substances such as cotton, filter paper possess unique structural hierarchies from macro- to molecular scales, as well as porous network structures at nanometer levels, and they can be used as ideal template substrates for the fabrication of functional artificial nanostructured materials [17, 18]. Hierarchical porous structural TiO_2 [19], TiN [20], silica [21] and SnO_2 [22] have been prepared using natural cellulose substances as template, and the resulting products with unique structure shows good performances on catalysis and/or electrochemical area. In this paper, a binary metal oxide $ZnMn_2O_4$ has been synthesised using absorbent cotton as template, and the structures, morphologies, particle sizes and electrochemical properties of as-prepared products are comparatively investigated and discussed in the context.

2. Experimental

2.1. Synthesis of hierarchical porous $ZnMn_2O_4$: The $ZnMn_2O_4$ is prepared by a simple cotton template route described as follow. 0.4958 g $Zn(NO_3)_2{\cdot}6H_2O$, 1.1930 $Mn(NO_3)_2$ (50 wt% in solution) and 1.0507 g citric acid are dissolved into 20 ml distilled water. Then, ~1.0 g of absorbent cotton is immersed into above solution. After drying at 80 °C for 1 day, the cotton-metal ion composition is at calcinated 600 °C for 4 h to obtain $ZnMn_2O_4$.

2.2. Structural characterisation: The crystal phases were measured on a powder X-ray diffractometer (DX-2700, Dandong) with Cu-Kα radiation (40 kV, 30 mA) and 0.03° in the 2θ range of 10 and 80°. The morphology and size were observed using JEOL JSM-7500F scanning electron microscope (SEM, 5 kV) and JEM-2100F transmission electron microscope (TEM, 100 kV). Specific surface area and corresponding pore size of $ZnMn_2O_4$ sample were measured using a Micromeritics ASAP 2020 sorptometer.

2.3. Electrochemical characterisation: CR 2016 coin cells of $ZnMn_2O_4$/Li are used for electrochemical experiments performed at 30 °C. The working electrodes were prepared as the following: after the mixing of electrode materials, acetylene black and binder sodium alginate at a weight ratio of 70:20:10, the resulting mixtures were slurried with water, pasted onto copper foils, and then dried at 80 °C for 5 h, cut into discs with diameter of 14 mm. Polymer (Celgard2400) and commercial LBC 301 $LiPF_6$ solution (Shenzhen CAPCHEM) were used as separators and electrolyte. The cells were assembled in an argon-filled glove box. The galvanostatic cycling tests were conducted on a CT-3008 battery test system (Shenzhen Neware) at various current rates between 0.01 and 3.0 V. Cyclic voltammetry (CV) studies were conducted on a CHI660B Electrochemical Workstation (Shanghai Chenhua) at a scanning rate of 0.2 mV s^{-1} between 3.0 and 0.01 V.

3. Results and discussion: The formation process of $ZnMn_2O_4$ derived from cotton substance is presented in Fig. 1. Initially, a ball of white cotton (~1 g) is soaked into as-prepared mixed solution, and the cotton will completely adsorb the solution. Then, the adsorbent is dried at 80 °C, and a ball of yellow metal ion-cotton composite (Fig. 1) can be obtained. After calcination of the composite at 600 °C, the overall structure has not been changed except the yellow is transformed into brown (Fig. 1).

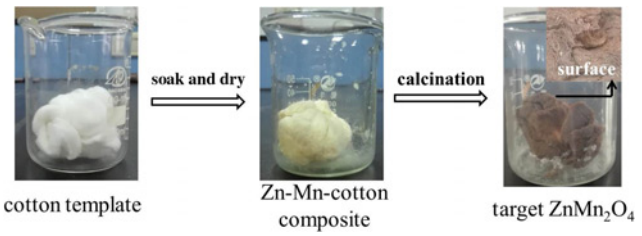

Fig. 1 *Graphic formation process of hierarchical porous $ZnMn_2O_4$, the inserted clearly indicates fibre-like structure of target $ZnMn_2O_4$*

Interestingly, some fibre-like structure of target product can be observed on the surface, which is similar to the cotton fibre, indicating the successful template effect of cotton substance.

After grinding the brown in an agate mortar, the obtained powder is firstly tested by XRD, and the pattern is shown in Fig. 2. All of diffraction peaks can be assigned to tetragonal $ZnMn_2O_4$ with space group $I4_1/amd$ (JCPDS Card No. 24-1133), and without any impurities such as ZnO and/or Mn_2O_3 can be detected, suggesting the cotton template route can be used to prepare binary metal oxide. Moreover, the sharp and strong peaks indicating the sample should be well constructed [9].

The morphology and surface structure of as-prepared $ZnMn_2O_4$ is studied using SEM, and the result is shown in Fig. 3. In an overall view (Fig. 3*a*), the sample generally show the bend fibre-like structure, which should be attributed to the template effect of cotton. In a magnification view (Fig. 3*b*), it can be seen the surface of $ZnMn_2O_4$ is not smooth, and some broken and helix structure can be found. Interestingly, in a further magnification view (Fig. 3*c*), some curving plate-like structure can be found. Maybe, partial coating of metal ions on the surface of cotton fibre may lead to the formation of curving plate structure. Moreover, in a close view (Fig. 4*d*), the plate-like $ZnMn_2O_4$ is composed of numerous nanosized particles. Thus, the as-prepared $ZnMn_2O_4$ can be defined as hierarchical materials.

To further investigate the structures and morphologies of as-prepared sample, the TEM, HR-TEM and SAED tests have been carried out for this $ZnMn_2O_4$. A thin plate is successfully captured in Fig. 4*a*. This plate is consisted of numerous nanoparticles, which is consistent with SEM observation. In a magnification image (Fig. 4*b*), it can be found that these nanoparticles with size of ~20–50 nm have clear edge and corner, suggesting the particles should be well crystallised [5]. In Fig. 4*c*, the lattice fringes with a spacing of 0.282 or 0.304 nm can be assigned to the (112) or (200) crystal face of tetragonal $ZnMn_2O_4$, and the interfacial angle between them was estimated to be ~59°, which is close to the

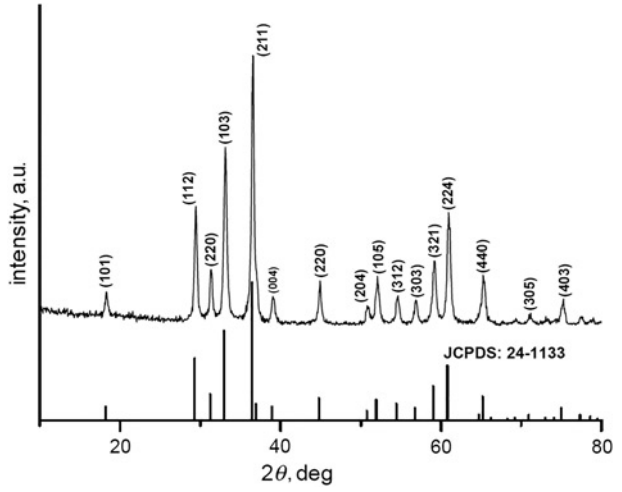

Fig. 2 *XRD pattern of $ZnMn_2O_4$ derived from cotton substance*

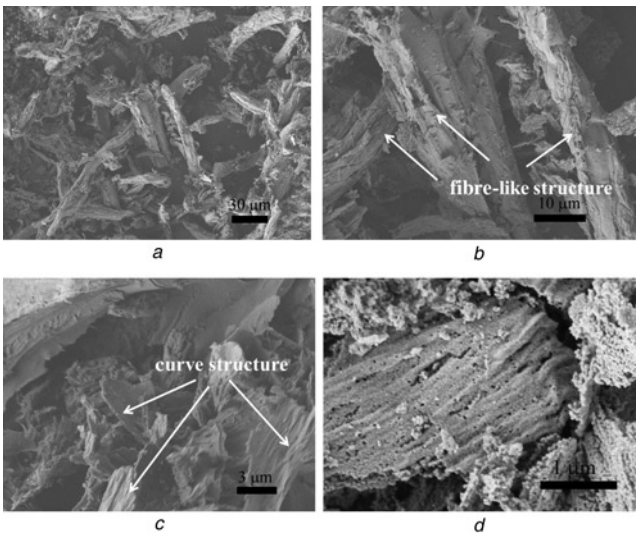

Fig. 3 *SEM images of $ZnMn_2O_4$ derived from cotton*
a Overall view
b, *c* and *d* Close view

theoretical data (~57.9°). The SAED pattern (Fig. 4*d*) shows the single-crystalline nature of independent nanoparticle, and some diffraction dots such as (112), (204) and (224) peak can be clearly presented, which can be indexed to the XRD pattern in Fig. 2.

The porous nature of as-prepared hierarchical $ZnMn_2O_4$ is proved by N_2 adsorption–desorption isotherms and pore size distribution pattern, as shown in Fig. 5. It is found that the $ZnMn_2O_4$ has a Brunauer–Emmett–Teller surface area of ~16.7084 $m^2 g^{-1}$, which is close to the reported literatures [11, 12]. An inset is the corresponding pore size distribution approximately estimated by Barrett–Joyner–Halenda method. The pore size covers the range from several nanometer to ~100 nm, giving an average pore diameter of ~27.0 nm.

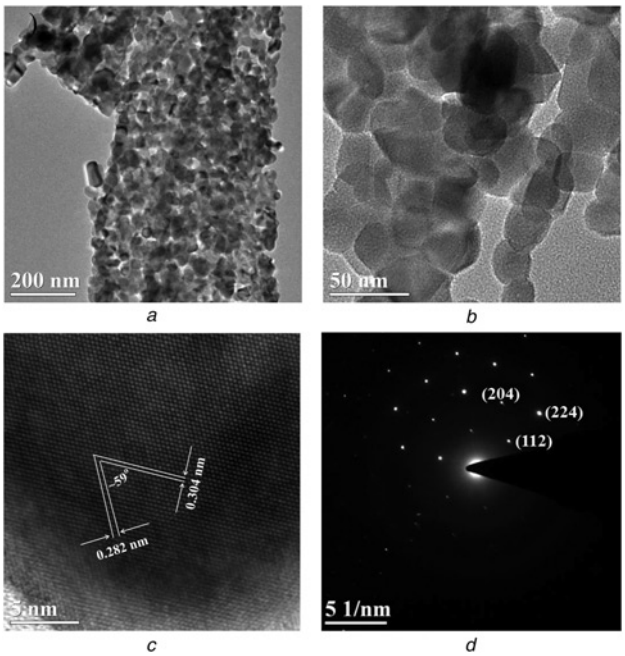

Fig. 4 *Close view of the plate-like $ZnMn_2O_4$ is composed of numerous nanosized particles*
a, *b* TEM
c HR-TEM
d SAED images of hierarchical $ZnMn_2O_4$ derived from cotton

doi: 10.1049/mnl.2016.0086

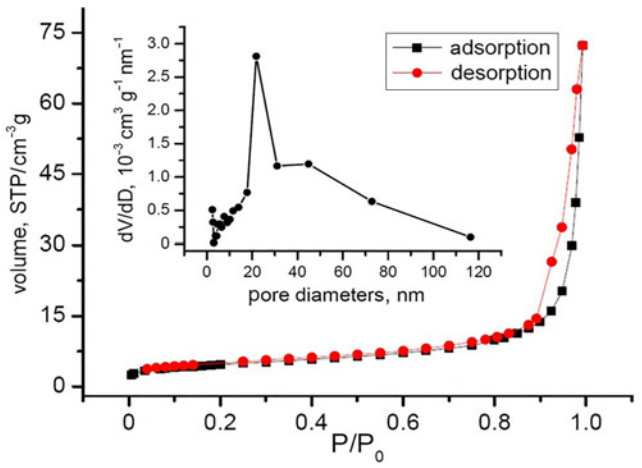

Fig. 5 *N_2 adsorption–desorption isotherms and an inserted pore size distribution of hierarchical porous $ZnMn_2O_4$*

As lithium ion battery anode, the electrochemical performances of hierarchical porous $ZnMn_2O_4$ are clearly studied. Fig. 6*a* reveals the typical discharge–charge curves at current density of 200 mA g^{-1} within 0.01–3.0 V. The hierarchical porous $ZnMn_2O_4$ deliver an initial discharge capacity of 1227.4 mAh g^{-1}, and reversible charge discharge 796.0 mAh g^{-1}, correspondingly giving the initial Coulombic efficiency of 64.9%. Fig. 4*b* shows the initial three CV curves of $ZnMn_2O_4$/Li cells at the scanning rate of 0.2 mV s^{-1} between 0.01 and 3.0 V. In the first discharge curve, the unique strong peak at 0.067 V is the reduction of $ZnMn_2O_4$ to metallic Mn, Zn and Li-Zn alloy. There are two anodic peaks located at 1.35 and 1.95 V in the first charge curve, which are associated with the formation of MnO and ZnO, respectively. From the second cycle onward, the repeated oxidation/reduction of MnO and ZnO leads to two pairs of redox peak at 0.49/1.24 and ~0.65/1.19 V, respectively [11–14].

The cycling stability of hierarchical porous $ZnMn_2O_4$ is studied in Fig. 6*c*. The second reversible discharge capacity is 789.3 mAh g^{-1}. Then, the discharge capacity decreases to 692.6 mAh g^{-1} at the 23th cycle. Afterward, the discharge capacity increases to a maximum value of 871.9 mAh g^{-1} at 70th cycle. After that, the capacity slowly decreases to 674.9 mAh g^{-1} at 200th cycle. Combination with the discharge–charge curves in Fig. 6*a*, the increasing discharge capacity within 23th–70th cycle may generally be attributed to the reversible formation of a polymeric gel-like film originating from kinetic activation in the electrode, which leads to capacity contribution increases in the voltage region of 2.0–3.0 V. In comparison with other literatures, this discharge capacity and cycling stability of as-prepared hierarchical porous $ZnMn_2O_4$ is not bad [5–9]. The good electrochemical properties of the porous nanowires are mainly ascribed to its porous structure not only provides electron transport paths and large contact area between the electrode and electrolyte, but also can efficiently accommodate the huge volume variations which is derived from the repeated lithium ions diffuse into/extraction the electrode [11].

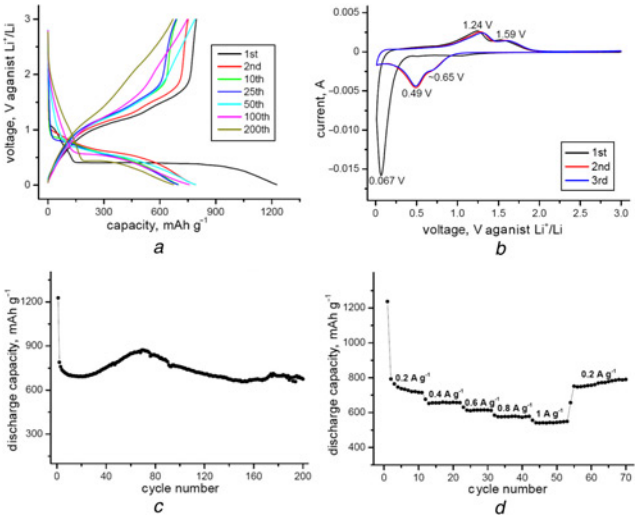

Fig. 6 *Electrochemical performances of as-prepared hierarchical porous $ZnMn_2O_4$*
a Typical discharge–charge curves
b CV profiles of the initial three cycles
c Cycling stability at 200 mA g^{-1}
d Rate capability at different current density

The rate capability of this $ZnMn_2O_4$ is also evaluated at different current densities, as shown in Fig. 6*d*. As expected, the specific capacity decreases from 792.7 mAh g^{-1} at 200 mA g^{-1} to 576.3 mAh g^{-1} at 800 mA g^{-1}, even when the current density increases to 1000 mA g^{-1}, the cell also delivers stable discharge capacity of about 541.5 mAh g^{-1}. Importantly, when current density goes back to 200 mA g^{-1}, the 55th cycle discharge capacity returns to a high value of 750.5 mAh g^{-1}. These results indicate the hierarchical porous $ZnMn_2O_4$ are suitable for high-rate Li ions storage processes.

4. Conclusion: A facile cotton template route has been successfully developed for the synthesis of binary metal oxide $ZnMn_2O_4$. Most of sample composed of numerous well-defined nanoparticles possess the fibre-like structure, and the porous nature is well proved by N_2 adsorption–desorption test. As lithium ion battery anode, this $ZnMn_2O_4$ deliver an initial discharge capacity of 1227.4 mAh g^{-1}, and reversible charge discharge 796.0 mAh g^{-1}. After 200 cycles, a high discharge capacity of 674.9 mAh g^{-1} can be retained. Maybe, the cotton template also can be used to prepare high-quality other binary metal oxides such as $CoMn_2O_4$ and $ZnCo_2O_4$, deserved to be conducted continuously.

5. Acknowledgment: The authors thank the financial supports from the Scientific Start Foundation of LongYan University (grant no. LB2014001), from the Innovative Training Program of Undergraduate (grant no. 201511312014).

6 References

[1] Poizot P., Laruelle S., Grugeon S., *ET AL.*: 'Nano-sized transition-metal oxides as negative-electrode materials for lithium-ion batteries', *Nature*, 2000, **407**, pp. 496–499
[2] Wang Z.Y., Zhou L., Lou X.W.: 'Metal oxide hollow nanostructures for lithium-ion batteries', *Adv. Mater.*, 2012, **24**, pp. 1903–1911
[3] Liu R., Yang W.D., Fang H.Y.: 'Performance of SnO_2/carbon nanotube composite electrode materials by the pechini method', *Micro Nano Lett.*, 2016, **11** pp. 54–56.
[4] Dai Y.H., Jiang H., Yu Y.J., *ET AL.*: 'Hydrothermal synthesis of hollow Mn_2O_3 nanocones as anode material for Li-ion batteries', *RSC Adv.*, 2013, **3**, pp. 19778–19781
[5] Yang Y.Y., Zhao Y.Q., Xiao L.F., *ET AL.*: 'Nanocrystalline $ZnMn_2O_4$ as a novel lithium-storage material', *Electrochem. Commun.*, 2008, **10**, pp. 1117–1120
[6] Xia L.F., Yang Y.Y., Yin J., *ET AL.*: 'Low temperature synthesis of flower-like $ZnMn_2O_4$ superstructures with enhanced electrochemical lithium storage', *J. Power Sources*, 2009, **194**, pp. 1089–1093
[7] Zhang G.Q., Yu L., Wu H.B., *ET AL.*: 'Formation of $ZnMn_2O_4$ ball-in-ball hollow microspheres as a high-performance anode for lithium-ion batteries', *Adv. Mater.*, 2012, **24**, pp. 4609–4613
[8] Zhou L., Wu H.B., Zhu T., *ET AL.*: 'Facile synthesis of $ZnMn_2O_4$ hollow microspheres as high-capacity anodes for lithium-ion batteries', *J. Mater. Chem.*, 2012, **22**, pp. 827–829
[9] Kim S.W., Lee H.W., Muralidharan P., *ET AL.*: 'Electrochemical performance and *ex situ* analysis of $ZnMn_2O_4$ nanowires as anode materials for lithium rechargeable batteries', *Nano Res.*, 2011, **4**, pp. 505–510
[10] Yang G.R., Xu X., Yang W., *ET AL.*: 'Facile synthesis of interwoven $ZnMn_2O_4$ nanofibers by electrospinning and their performance in Li-ion batteries', *Mater. Lett.*, 2014, **128**, pp. 336–339

[11] Zhang Y.H., Zhang Y.W., Guo C.L., *ET AL.*: 'porous $ZnMn_2O_4$ nanowires as an advanced anode material for lithium ion battery', *Electrochim. Acta*, 2015, **182**, pp. 1140–1144
[12] Zhang L.X., Wang Y.L., Jiu H.F., *ET AL.*: 'Hollow core-shell $ZnMn_2O_4$ microspheres as a high-performance anode material for lithium-ion batteries', *Ceramics Int.*, 2015, **41**, pp. 9655–9661
[13] Deng Y.F., Wang L.N., Xie Y., *ET AL.*: 'Recent advance in Mn-based oxides as anode materials for lithium ion batteries', *RSC Adv.*, 2014, **4**, pp. 23914–23935
[14] Wu F.F., Bai J., Feng J.K., *ET AL.*: 'Porous mixed metal oxides: design, formation mechanism and application in lithium-ion batteries', *Nanoscale*, 2015, **7**, pp. 17211–17230
[15] Chen X.F., Qie L., Zhang L.L., *ET AL.*: 'Self-templated synthesis of hollow porous submicron $ZnMn_2O_4$ sphere as anode for lithium-ion batteries', *J. Alloy Compd.*, 2013, **559**, pp. 5–10
[16] Wang N.N., Ma X.J., Xu H.Y., *ET AL.*: 'Porous $ZnMn_2O_4$ microspheres as a promising anode material for advanced lithium-ion batteries', *Nano Energy*, 2014, **6**, pp. 193–199
[17] Jia D.L., Wang M.Y., Li S., *ET AL.*: 'Functional nanostructured materials template by natural cellulose substance', *Chin. Sci. Bull.*, 2014, **59**, pp. 1369–1381
[18] Hall S.R., Bolger H., Mann S.: 'Morphosynthesis of complex inorganic forms using pollen grain templates', *Chem. Commun.*, 2003, **39**, pp. 2784–2785
[19] Zhao J., Gu Y.Q., Huang J.G.: 'Flame synthesis of hierarchical nanotubular rutile titania derived from natural cellulose substance', *Chem. Commun.*, 2011, **47**, pp. 10551–10553
[20] Lin X.Y., Zhang Y.H., Wu T., *ET AL.*: 'Hierarchical nanotubular titanium nitride derived from natural cellulose substance and its electrochemical properties', *Chem. Commun.*, 2012, **48**, pp. 9992–9994
[21] Zhang Y.H., Liu X.Y., Huang J.G.: 'Hierarchical mesoporous silica nanotubes derived from natural cellulose substance', *ACS Appl. Mater. Interfaces*, 2011, **3**, pp. 3272–3275
[22] Huang J.G., Matsunaga N., Shimanoe K., *ET AL.*: 'Nanotubular SnO_2 templated by cellulose fibers: synthesis and gas sensing', *Chem. Mater.*, 2005, **17**, pp. 3513–3518

doi: 10.1049/mnl.2016.0086